

Full paper / Mémoire

# Formation of naphthodithiophene isomers by flash vacuum pyrolysis of 1,6-di(2-thienyl)- and 1,6-di(3-thienyl)-1,5-hexadien-3-yne

Rui Umeda, Hiroshi Fukuda, Koji Miki<sup>1</sup>, S. M. Abdur Rahman<sup>2</sup>, Motohiro Sonoda<sup>3</sup>, Yoshito Tobe\*

*Division of Frontier Materials Science, Graduate School of Engineering Science, Osaka University, 1-3 Machikaneyama, Toyonaka 560-8531, Japan*

Received 5 June 2008; accepted after revision 18 September 2008  
Available online 28 November 2008

## Abstract

To develop a synthetic method of thiophene-based polycyclic aromatic compounds, we investigated the tandem cyclization of 1,6-dithienyl-1,5-hexadien-3-yne under flash vacuum pyrolysis (FVP) conditions at high temperatures (850 or 1050 °C). As a result, several isomeric naphthodithiophene derivatives were obtained as mixtures, from which a few isomers were isolated. The structural assignments of the products were performed on the basis of combination of the experimental and calculated <sup>1</sup>H NMR chemical shifts of either purified products or mixtures of them. Plausible mechanisms for the formation of the products are proposed. **To cite this article:** R. Umeda *et al.*, *C. R. Chimie* 12 (2009).

© 2008 Académie des sciences. Published by Elsevier Masson SAS. All rights reserved.

**Keywords:** Flash vacuum pyrolysis; Cyclization; Naphthodithiophenes; C–C bond formation

## 1. Introduction

Thiophene-based polycyclic aromatic compounds, linearly fused systems in particular, have been attracting a great deal of interest in view of application to organic

materials for electronic devices such as organic field-effect transistors (OFETs) and light emitting diodes (OLEDs) [1]. For instance, anthradithiophene, which is an isostructural analogue of pentacene, displayed improved solubility, robustness toward oxidative degradation, and solid-state ordering in favor of  $\pi$  stacking compared to pentacene [2]. Furthermore, Takimiya and coworkers reported that the extended benzothiophene derivatives showed good characteristics of OFETs [1b,3]. Compared to the linearly fused thiophene-based aromatics, little is known for angularly fused systems with regard to application to organic materials [4], presumably because they would exhibit larger HOMO–LUMO gaps than the linear systems.

For tetracyclic naphthodithiophenes, for example, of the 12 possible isomers shown in Fig. 1, which are

\* Corresponding author.

E-mail address: [tobe@chem.es.osaka-u.ac.jp](mailto:tobe@chem.es.osaka-u.ac.jp) (Y. Tobe).

<sup>1</sup> Present address: Department of Energy and Hydrocarbon Chemistry, Graduate School of Engineering, Kyoto University, Katsuma, Nishikyo-ku, Kyoto 615-8510, Japan.

<sup>2</sup> Present address: Department of Clinical Pharmacy and Pharmacology, Faculty of Pharmacy, University of Dhaka, Dhaka 1000, Bangladesh.

<sup>3</sup> Present address: Department of Applied Chemistry, Graduate School of Engineering, Osaka Prefecture University, 1-1 Gakuencho, Sakai 599-8531, Japan.

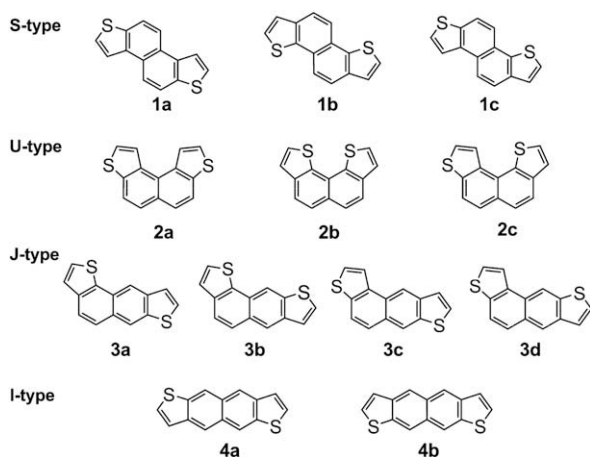
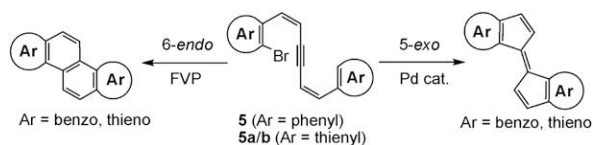


Fig. 1. Structures of naphthodithiophene isomers.

classified according to the molecular shapes as S-, U-, J-, and I-types, only three of them, naphtho[2,1-b:6,5-b']dithiophene (**1a**), naphtho[2,1-b:7,8-b']dithiophene (**2a**), and naphtho[1,2-b:8,7-b']dithiophene (**2b**), are known [5]. However, although their synthesis was reported, their physical data are not cited. We report herein the synthesis of some of the naphthodithiophenes using flash vacuum pyrolysis (FVP) of readily available dithienyldienynes [6].

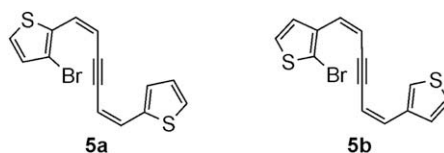
As a part of our work on the synthesis of new polycyclic aromatic compounds based on tandem cyclization including alkyne linkages, we reported that flash vacuum pyrolysis (FVP) of diphenylhexadienynes derivative having a bromine atom **5** (Ar = phenyl) gave chrysene as a major product by 6-*endo* cyclization at high temperatures (Scheme 1, left) [7]. In contrast, we also found that palladium-catalyzed cyclization of **5** (Ar = phenyl) gave the biindenylidene derivatives as a sole product by 5-*exo* cyclization (Scheme 1, right) [8a]. Similarly, Pd-catalyzed cyclization worked well with the thiophene derivatives **5a** and **5b** (Fig. 2), producing cyclopentene-fused dithienylethenes [8b]. It is therefore usual to extend our work to FVP of **5a** and **5b** with an expectation of the formation of naphtho[2,1-b:6,5-b']dithiophene (**1a**) and naphtho[1,2-b:5,6-b']dithiophene (**1b**) as the major products, respectively. We found, however, the results were more complicated

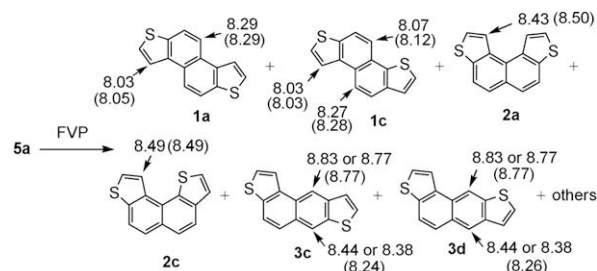
Scheme 1. 5-Exo and 6-endo tandem cyclizations of **5**.

because of not only the two different reaction centers,  $\alpha$  and  $\beta$  positions, in the thiophene ring but also the less selective 6-*endo* cyclization mode, leading to the formation of mixtures of isomers. From the mixtures, new compounds **1c** and **2c** were isolated in pure forms and fractions containing **1a** and **1b** as each major component were also obtained (Fig. 1).

## 2. Results and discussion

The substrates of FVP **5a** and **5b** were prepared by the previous method developed by our group [8b]. First, we carried out FVP of **5a** at 850 °C (Scheme 2). In contrast to the FVP of **5** (Ar = phenyl) [7], the reaction of **5a** afforded a complex mixture of products as indicated by the <sup>1</sup>H NMR spectrum of the crude product (Fig. S2). The crude product was subjected to GPC separation, giving two fractions A and B. From the first fraction A, one of major products was isolated, of which structure assignment is outlined below. The <sup>1</sup>H NMR spectrum (Fig. S3) exhibits eight doublets and the <sup>13</sup>C NMR spectrum shows 14 signals. These results indicate the product has an unsymmetrical structure such as **1c** or **2c** (Fig. 1). The most characteristic feature of the <sup>1</sup>H NMR spectrum of this product is the remarkable low field shift of two naphthalene protons which appear at 8.27 (d, *J* = 8.7 Hz, 1H) and 8.07 (d, *J* = 8.8 Hz, 1H) ppm and one thiophene proton which appears at 8.03 (d, *J* = 5.4 Hz, 1H) ppm owing to the anisotropic deshielding effect, indicating that these protons are located in the *bay* region. Among the possible products shown in Fig. 1, only **1c** fits the observed NMR spectra. Moreover, the deshielded chemical shifts agree well with the calculated values (8.28, 8.12, and 8.03 ppm, respectively) obtained by the GIAO method at the B3LYP/6-31g(d,p)//B3LYP/6-31g(d,p) level (Scheme 2 and Fig. S4). The second GPC fraction B contained at least five products as indicated by the <sup>1</sup>H NMR spectrum (Fig. S5) and GC analysis. Moreover, GC mass spectrum of the major peaks of this fraction exhibited molecular ions corresponding to the naphthodithiophenes (*m/z* 240), indicating the absence of fragmentation to small fragments. The fraction B was separated by column

Fig. 2. Precursors **5a** and **5b** for FVP.



Scheme 2. The structures of the products of FVP of **5a** and the observed  $^1\text{H}$  NMR chemical shifts. Values in parentheses are the calculated chemical shifts by GIAO-B3LYP/6-31g(d,p)//B3LYP/6-31g(d,p) method.

chromatography on aluminum oxide, giving a fraction (B1) consisting of a sole product and a fraction (B2) containing another product as a major component. The  $^1\text{H}$  NMR spectrum of fraction B1 (Fig. S6) also shows eight doublets, indicating that this compound possesses an unsymmetric structure. In this case, however, only one low field-shifted signal for a thiophene proton was observed at 8.49 (dd,  $J = 0.7, 5.4$  Hz, 1H), indicating that this compound contains one thiophene proton in the bay region. Accordingly, we assign this compound as compound **2c**. This assignment is also supported by the calculated NMR shift (8.49 ppm) for the thiophene proton (Scheme 2 and Fig. S4). Analysis of the  $^1\text{H}$  NMR spectrum of the other fraction B2 (Fig. S7) allowed us the assignment of its major component to **1a**; it shows four doublet signals, consistent with a symmetrical structure, with two of which (for naphthalene protons at 8.29 (d,  $J = 8.5$  Hz, 2H) ppm and for thiophene protons at 8.03 (d,  $J = 5.5$  Hz, 2H) ppm) being observed at low field due to the anisotropic deshielding effect. The calculated NMR chemical shifts of the above protons of **1a** (8.29 and 8.05 ppm, respectively) agree well with the observed ones (Scheme 2 and Fig. S4).

Although we could not isolate other products or obtain fractions enriched with the others, the structures of the other minor products were assumed on the basis of the  $^1\text{H}$  NMR spectrum of the fraction B before subjection to column chromatography (Fig. S5). It exhibits the characteristic two pair of singlet signals at relative low field (8.38 and 8.77 ppm, 8.44 and 8.83 ppm). One of the signal in the each pair is subject to strong anisotropic deshielding effect. In addition to the spectroscopic data, the fact that in the case of **5** (Ar = phenyl), J-shaped product, benz[*a*]anthracene, was formed as a minor product led us to assume that the structures of the minor products to be **3c** and **3d** (Scheme 2 and Fig. S4). Also, the formation of

compound **2a** was suggested from the  $^1\text{H}$  NMR spectrum of the crude product, which exhibited the thiophene proton at 8.43 ppm located at the bay region (Scheme 2 and Fig. S4).

The product distribution was determined by the integral ratio of characteristic signals in the  $^1\text{H}$  NMR spectrum of the crude product of FVP of **5a** (Fig. S2). The results at higher temperature (1050 °C) are also listed in Table 1. As shown, the distribution of products was not affected by changing the temperature from 850 °C to 1050 °C, indicating the absence of equilibrium between the products.

Next, we carried out FVP of **5b**. In this case, several products were formed too (Scheme 3 and Fig. S8). In the same manner as the purification of the products of **5a**, the mixtures were separated by GPC and the structures were assigned on the basis of  $^1\text{H}$  NMR spectra. First, by separation of the crude products by GPC, three fractions (fractions C–E) were obtained. One of them, fraction C, was identified as compound **1c**, because its  $^1\text{H}$  NMR data (Fig. S9) were identical with the one obtained from pyrolysis of **5a**. The  $^1\text{H}$  NMR spectrum of the second GPC fraction D (Fig. S10) shows four doublets indicating **1b** or **2b** as the candidate among the possible structures (Fig. 1). In addition, since the signal of a naphthalene proton is observed at relatively low field of 8.06 (d,  $J = 8.4$  Hz, 1H) ppm, we assume this compound to be **1b**. The third GPC fraction E is assumed to contain two major compounds on the basis of the  $^1\text{H}$  NMR spectrum (Fig. S11). One of them was identified to be **2c** by comparison of the  $^1\text{H}$  NMR data with that observed in the pyrolysate of **5a**. The other component shows four doublet signals which are not subject to the anisotropic

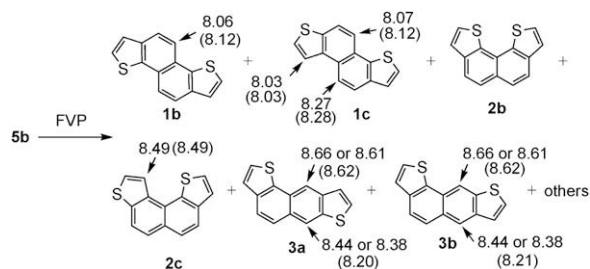
Table 1  
Product distribution by FVP of **5a** and **5b**<sup>a</sup>

	Temperature [°C]	Balance <sup>b</sup> [%]	Product distribution (%) <sup>c</sup>					
			<b>1a</b>	<b>1c</b>	<b>2a</b>	<b>2c</b>	<b>3c</b>	<b>3d</b>
<b>5a</b>	850	55	27	27	14	22	5	5
	1050	45	30	25	12	21	6	6
<b>5b</b>	850	54	<b>1b</b>	<b>1c</b>	<b>2b</b>	<b>2c</b>	<b>3a</b>	<b>3b</b>
	1050	48	33	22	15	15	7.5	7.5
			33	23	17	13	7	7

<sup>a</sup> The reactions were carried out at ca. 1 mmHg under a slow stream of Argon which was introduced through a capillary into the pyrolysis tube (see Supplementary material for the detail).

<sup>b</sup> Percent ratio of the weight of products relative to the starting material which passed through the hot zone of the pyrolysis tube assuming that all products have the same molecular formula  $\text{C}_{14}\text{H}_8\text{S}_2$ .

<sup>c</sup> Based on the integral ratio of characteristic signals in the  $^1\text{H}$  NMR spectrum of crude reaction product after FVP.



Scheme 3. The structures of the products of FVP of **5b** and the observed  $^1\text{H}$  NMR chemical shifts. Values in parentheses are the calculated chemical shifts by GIAO-B3LYP/6-31g(d,p)//B3LYP/6-31g(d,p) method.

deshielding, indicating that this compound has a symmetrical structure and does not possess any proton in the *bay* region. These observations suggest that this compound is **2b**. This is supported by the calculated NMR chemical shifts (Fig. S12). In addition, the  $^1\text{H}$  NMR spectra of all fractions C–E exhibit the characteristic pair of singlet signals (8.38 and 8.66 ppm, 8.44 and 8.61 ppm) of low intensities at relatively low field, indicating the presence of J-type compounds such as **3a** and **3b** (Figs. S9–S11).

The results of FVP of **5b** at both 850 °C and 1050 °C are listed in Table 1. Similarly to the case of **5a**, the distribution of the products produced from **5b** was not affected by temperature, indicating that the products are formed under kinetic control.

The relative energy of the equilibrium geometry of naphthodithiophenes **1–4** calculated by using B3LYP method with 6-31G(d,p) basis set is shown in Table 2. Within the individual type isomers **1**, **3**, and **4**, the relative energies are not much different. However, the case of U-type isomers **2a–c**, the relative enthalpies are dependent on the position of sulfur atoms due to steric and electronic reasons. Moreover, the relative energies are also affected by the positions of fusion. The S-type products **1a–c**, which were obtained as major products from **5a** and **5b**, were shown to possess relatively high energies. These results also implied that the formation of the naphthodithiophene products was conducted under kinetic control.

The trend of product distributions is consistent with that of FVP of **5** (Ar = phenyl), though two products such as **1c** and **2c** were formed as S-type products by FVP of **5a** and **5b** because of the unsymmetrical structure of thiophene ring. For example, in the case of the FVP of **5** (Ar = phenyl) at 800 °C, the products were obtained in the following ratio, S-type (73%), U-type (21%), and J-type (6%) [7]. The selectivity to S-type products from **5a** and **5b** was slightly low as

Table 2

Comparison of the relative energies of the equilibrium geometries of naphthodithiophenes **1–4** calculated by using the B3LYP method with the 6-31G(d,p) basis set

Type	Compound	$E(\text{RB} + \text{HF} - \text{LYP})$ (hartree)	$E$ (kcal/mol) <sup>a</sup>	$\Delta E$ (kcal/mol) <sup>b</sup>
S	<b>1a</b>	-1334.71720644	-837547.7269	-0.405
	<b>1b</b>	-1334.71785138	-837548.1316	0
	<b>1c</b>	-1334.71748486	-837547.9016	-0.230
U	<b>2a</b>	-1334.71276953	-837544.9427	-3.19
	<b>2b</b>	-1334.71654431	-837547.3114	-0.820
	<b>2c</b>	-1334.71583929	-837546.869	-1.26
J	<b>3a</b>	-1334.71475090	-837546.186	-1.95
	<b>3b</b>	-1334.71441062	-837545.9725	-2.16
	<b>3c</b>	-1334.71434996	-837545.9344	-2.20
	<b>3d</b>	-1334.71428595	-837545.8942	-2.24
I	<b>4a</b>	-1334.70941672	-837542.8387	-5.29
	<b>4b</b>	-1334.70932978	-837542.7842	-5.35

<sup>a</sup> 1 hartree = 627.5095 kcal/mol.

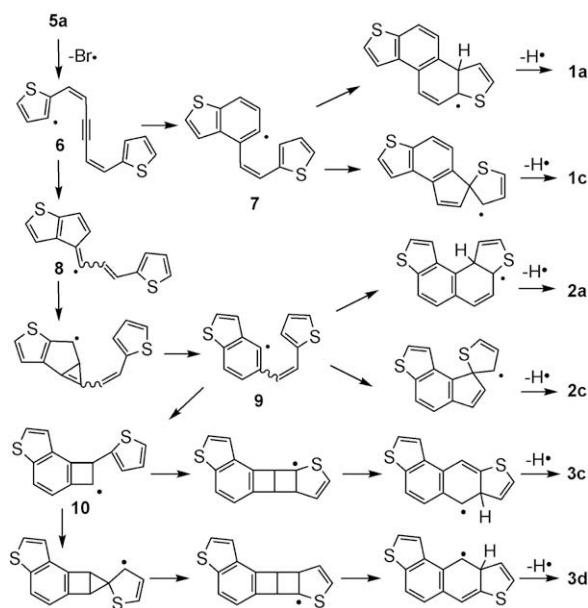
<sup>b</sup> Relative energy based on compound **1b**.

compared to that of **5** (Ar = phenyl), the reason of which is described later. In both cases with **5a** and **5b**, the material balance at 1050 °C was slightly lower than that at 850 °C presumably because of the greater possibility of degradation of the intermediate species of cyclization.

### 3. Plausible mechanism of the formation of the naphthodithiophene derivatives

Plausible mechanisms of the formation of the naphthodithiophene derivatives **1a**, **1c**, **2a**, **2c**, **3c**, and **3d** are shown in Scheme 4. Obviously, at the high temperature,<sup>4</sup> the homolytic cleavage of the C–Br bond should be the initial event [9], leading to the formation of radical species **6**. Then, the generated radical **6** would form the benzothiophene radical species **7** by 6-*endo* cyclization. Subsequent 6-*endo* cyclization at  $\beta$ -position of the thiophene ring followed by elimination of hydrogen would afford compound **1a**. On the contrary, 6-*endo* cyclization at  $\alpha$ -position of the thiophene ring followed by the ring expansion would form compound **2c**. On the other hand, 5-*exo* cyclization of the initially formed radical **6** to form **8** and subsequent three-membered cyclization and ring expansion would give another benzothiophene radical species **9**. The formation of compounds **2a** and **2c** can

<sup>4</sup> At lower pyrolysis temperature (650 °C), the isomers of the substrate **5a** such as (*E,E*), (*E,Z*), and (*Z,E*) isomers were also obtained together with recovered **5a** and the pyrolysis products, which were identified in the  $^1\text{H}$  NMR spectrum of the crude product.



Scheme 4. A plausible mechanism of formation of naphthodithiophene derivatives **1a**, **1c**, **2a**, **2c**, **3c**, and **3d** produced by FVP of **5a**.

be explained in terms of the same cyclization assumed for **1a** and **1c** from **7**. In order to explain the formation of **3c** and **3d**, however, one should assume the formation of cyclobutyl radical intermediate **10** from **9**. Thus compounds **3c** and **3d** might be formed from **10** through intermediates having highly strained bicyclo[2.1.0]pentane and bicyclo[2.2.0]hexane structures. Though they look peculiar in view of the strain, a similar intermediate has been proposed in the literature for the FVP of 3-(2-thienonyl)cinnoline [6d]. The mechanism is based on conjecture: it would be confirmed by DFT calculation of the intermediates, which is the topic of our future research. The relatively low product distribution of S-type products **1a** and **1c** from **5a** compared to that of chrysene from **5** (Ar = phenyl) can be ascribed to the slower rate of the initial 6-*endo* cyclization relative to 5-*exo* mode owing to the smaller bond angle of the thiophene ring in intermediate **6**. The formation of **1b**, **1c**, **2b**, **2c**, **3a**, and **3b** produced by FVP of **5b** could be explained in the same manner (see [Supplementary material](#)).

#### 4. Conclusion

In conclusion, FVP of **5a** and **5b** gave a mixture of naphthodithiophene isomers **1a–c**, **2a–c**, and **3a–d**, from which **1b**, **1c**, and **2c** were isolated in almost pure state. Their structures were elucidated on the basis of

the observed and calculated  $^1\text{H}$  NMR spectra. The formation of the other products is assumed on the basis of  $^1\text{H}$  NMR spectra of the crude and partly purified products.

## 5. Experimental details

### 5.1. General

For FVP apparatus a ceramic electric furnace (Asahi Rika-Seisakusyo, ARF-30K) and a temperature control unit (Asahi Rika-Seisakusyo, AMF-N) were used.  $^1\text{H}$  NMR spectra were recorded on a Varian Mercury 300 spectrometer in  $\text{CDCl}_3$  and with  $\text{Me}_4\text{Si}$  or residual solvent as an internal standard at  $30^\circ\text{C}$ . IR spectra were recorded as KBr disks with a JASCO FTIR-410 spectrometer. Mass spectral analyses were performed on a JEOL JMS-700 spectrometer for EI ionization. GC/MS analysis was performed on a JEOL JMS-700 spectrometer coupled to a Agilent 6890 series (J&W Scientific HP-5 30 m  $\times$  0.320 mm). Column chromatography was performed with MERCK Aluminiumoxid 60 F254. Preparative GPC separation was undertaken with a JAILC-908 chromatograph using 600-mm  $\times$  20-mm JAIGEL-1H and 2H GPC columns with  $\text{CHCl}_3$  as an eluent. DFT calculations were performed with Gaussian 03 program package [10]. The geometries of the compounds were optimized by using the B3LYP method with the 6-31G(d,p) basis set. The nature of the stationary points was assessed by means of vibration frequency analysis. The chemical shifts were calculated by the GIAO-B3LYP/6-31G(d,p) method.

### 5.2. Experimental procedure of FVP

The schematic apparatus of FVP is shown in [Fig. S1](#). The hot zone consisting of a quartz tube was heated by an electric furnace to temperatures of  $850^\circ\text{C}$  or  $1050^\circ\text{C}$ . Under a slow stream of argon at reduced pressure (about 1 mmHg), a sample **5a** or **5b** (30 mg) was sublimed by heating with a heat-gun. The products passed through the hot zone were collected in a cold trap (liq.  $\text{N}_2$ ). After most of the sample was passed through the hot zone, heating was stopped. After cooling to room temperature, the products were collected by washing the quartz tube and the trap with  $\text{CHCl}_3$ . This procedure was repeated three times to obtain enough amount of products for analysis. The combined crude product was separated by GPC and column chromatography. The relative ratio of the products was estimated on the basis of the  $^1\text{H}$  NMR integration for the characteristic signals.

### 5.2.1. FVP of 5a

GPC separation gave fractions A (compound **1c**, 6 mg) and B (18 mg). Fraction B was subjected to column chromatography to give fraction B1 (compound **2c**, 4 mg) and B2 (mainly compound **1a**, 7 mg).  $^1\text{H}$  NMR spectrum of crude products before separation by GPC was shown in Fig. S2. Partial  $^1\text{H}$  NMR spectrum of fraction A (compound **1c**) is shown in Fig. S3.  $^1\text{H}$  NMR spectrum of fraction B before subjection to column chromatography is shown in Fig. S5. Partial  $^1\text{H}$  NMR spectra of fraction B1 (compound **2c**) and fraction B2 (mainly compound **1a**) are shown in Figs. S6 and S7, respectively. The calculated  $^1\text{H}$  NMR chemical shifts of **1a**, **1c**, **2a**, **2c**, **3c**, and **3d** are described in Fig. S4.

Compound **1c**: m.p. 139.0–140.0 °C,  $^1\text{H}$  NMR (400 MHz,  $\text{CDCl}_3$ , 30 °C)  $\delta$  8.27 (d,  $J = 8.7$  Hz, 1H), 8.07 (d,  $J = 8.8$  Hz, 1H), 8.03 (d,  $J = 5.4$  Hz, 1H), 8.00 (d,  $J = 8.8$  Hz, 1H), 7.97 (d,  $J = 8.7$  Hz, 1H), 7.64 (d,  $J = 5.4$  Hz, 1H), 7.53 (d,  $J = 5.3$  Hz, 1H), 7.50 (d,  $J = 5.3$  Hz, 1H);  $^{13}\text{C}$  NMR (75 MHz,  $\text{CDCl}_3$ , 30 °C)  $\delta$  138.2, 136.9, 136.8, 136.7, 126.4, 126.3, 126.2, 125.0, 124.8, 122.3, 122.2, 121.2, 120.9, 120.8; IR (KBr) 3098, 2923, 1651, 1556, 1514, 1465, 1415, 1365, 1340, 1293, 1187, 1161, 1101, 1086, 907, 882, 808, 732, 698, 606  $\text{cm}^{-1}$ ; MS (EI)  $m/z$  240 ( $\text{M}^+$ ).

Compound **2c**: m.p. 101.5–102.5 °C,  $^1\text{H}$  NMR (400 MHz,  $\text{CDCl}_3$ , 30 °C)  $\delta$  8.49 (dd,  $J = 5.7$ , 0.9 Hz, 1H), 8.01 (dd,  $J = 8.7$ , 0.7 Hz, 1H), 7.98 (d,  $J = 8.7$  Hz, 1H), 7.92 (d,  $J = 8.7$  Hz, 1H), 7.91 (d,  $J = 8.7$  Hz, 1H), 7.77 (d,  $J = 5.7$ , 0.9 Hz, 1H), 7.67 (d,  $J = 5.4$  Hz, 1H), 7.60 (d,  $J = 5.4$  Hz, 1H); MS (EI)  $m/z$  240 ( $\text{M}^+$ ).

Compound **1a**:  $^1\text{H}$  NMR (400 MHz,  $\text{CDCl}_3$ , 30 °C)  $\delta$  8.29 (d,  $J = 9.0$  Hz, 2H), 8.04 (d,  $J = 9.0$  Hz, 2H), 8.03 (d,  $J = 5.4$  Hz, 2H), 7.64 (d,  $J = 5.4$  Hz, 1H); MS (EI)  $m/z$  240 ( $\text{M}^+$ ).

### 5.2.2. FVP of 5b

GPC separation gave fractions C (compound **1c**, 7 mg), D (compound **1a**, 7 mg), and E (13 mg). Partial  $^1\text{H}$  NMR spectrum of fraction C (mainly **1c**) is shown in Fig. S6.  $^1\text{H}$  NMR spectrum of crude products before separation by GPC is shown in Fig. S8. Partial  $^1\text{H}$  NMR spectrum of C (mainly compound **1c**), fraction D (mainly compound **1b**), and fraction E (mainly compounds **2b** and **2c**) are shown in Figs. S9–S11, respectively. The calculated  $^1\text{H}$  NMR chemical shifts of **1b**, **2b**, **3a**, and **3b** are described in Fig. S12.

Compound **1b**:  $^1\text{H}$  NMR (300 MHz,  $\text{CDCl}_3$ , 30 °C)  $\delta$  8.06 (d,  $J = 8.4$  Hz, 1H), 7.94 (d,  $J = 8.4$  Hz, 1H),

7.53 (d,  $J = 5.1$  Hz, 1H), 7.49 (d,  $J = 5.1$  Hz, 1H); MS (EI)  $m/z$  240 ( $\text{M}^+$ ).

Compound **2b**:  $^1\text{H}$  NMR (300 MHz,  $\text{CDCl}_3$ , 30 °C)  $\delta$  8.02 (d,  $J = 8.1$  Hz, 1H), 7.97 (d,  $J = 8.1$  Hz, 1H), 7.77 (d,  $J = 5.4$  Hz, 1H), 7.65 (d,  $J = 5.4$  Hz, 1H).

## Acknowledgements

This work was supported by a Grant-in-Aid for Scientific Research on Priority Areas “Advanced Molecular Transformation of Carbon Resources” from the Ministry of Education, Culture, Sports, Science and Technology, Japan.

## Appendix. Supplementary material

Supplementary material associated with this article can be found, in the online version, at [doi:10.1016/j.crci.2008.09.020](https://doi.org/10.1016/j.crci.2008.09.020).

## References

- [1] For recent reviews, see: (a) J.E. Anthony, Chem. Rev. 106 (2006) 5028.  
(b) K. Takimiya, Y. Kunugi, T. Otsubo, Chem. Lett. 36 (2007) 578.
- [2] (a) J.G. Laquindanum, H.E. Katz, A.J. Lovinger, J. Am. Chem. Soc. 120 (1998) 664;  
(b) H.E. Katz, Z. Bao, J. Phys. Chem. B 104 (2000) 671.
- [3] (a) K. Takimiya, H. Ebata, K. Sakamoto, T. Izawa, T. Otsubo, Y. Kunugi, J. Am. Chem. Soc. 128 (2006) 12604.  
(b) K. Yamamoto, K. Takimiya, J. Am. Chem. Soc. 129 (2007) 2224.
- [4] A. Pietrangelo, M.J. MacLachlan, M.O. Wolf, B.O. Patrick, Org. Lett. 9 (2007) 3571.
- [5] (a) B.D. Tilak, Proc. Indian Acad. Sci. Sect. A 33 (1951) 71;  
(b) B.D. Tilak, Proc. Indian Acad. Sci. Sect. A 37 (1953) 114;  
(c) B.D. Tilak, Tetrahedron 9 (1960) 76;  
(d) D. Muller, J.-F. Muller, D. Cagniant, J. Chem. Res. (S) (1977) 328.
- [6] For some examples of the formation of the thiophene-based aromatic compounds by FVP, see: (a) M.L. Leow, J.A.H. MacBride, Tetrahedron Lett. 25 (1984) 4283;  
(b) R.A. Aitken, C. Boeters, J.J. Morrison, J. Chem. Soc. Perkin Trans. 1 (1997) 2625;  
(c) K. Imamura, D. Hirayama, H. Yoshimura, K. Takimiya, Y. Aso, T. Otsubo, Tetrahedron Lett. 40 (1999) 2789;  
(d) Y.A. Ibrahim, N.A. Al-Awadi, K. Kaul, Tetrahedron 57 (2001) 7377;  
(e) A. Brown, J.I.G. Cadogan, A.D. MacPherson, H. McNab, ARKIVOC xi (2007) 64.
- [7] M. Sonoda, K. Itahashi, Y. Tobe, Tetrahedron Lett. 43 (2002) 5269.
- [8] (a) S.M.A. Rahman, M. Sonoda, K. Itahashi, Y. Tobe, Org. Lett. 5 (2003) 3411;  
(b) S.M.A. Rahman, M. Sonoda, M. Ono, K. Miki, Y. Tobe, Org. Lett. 8 (2006) 1197.

- [9] L.T. Scott, *Angew. Chem. Int. Ed.* 43 (2004) 4994.
- [10] M.J. Frisch, G.W. Trucks, H.B. Schlegel, G.E. Scuseria, M.A. Robb, J.R. Cheeseman, J.A. Montgomery Jr., T. Vreven, K.N. Kudin, J.C. Burant, J.M. Millam, S.S. Iyengar, J. Tomasi, V. Barone, B. Mennucci, M. Cossi, G. Scalmani, N. Rega, G.A. Petersson, H. Nakatsuji, M. Hada, M. Ehara, K. Toyota, R. Fukuda, J. Hasegawa, M. Ishida, T. Nakajima, Y. Honda, O. Kitao, H. Nakai, M. Klene, X. Li, J.E. Knox, H.P. Hratchian, J.B. Cross, V. Bakken, C. Adamo, J. Jaramillo, R. Gomperts, R.E. Stratmann, O. Yazyev, A.J. Austin, R. Cammi, C. Pomelli, J.W. Ochterski, P.Y. Ayala, K. Morokuma, G.A. Voth, P. Salvador, J.J. Dannenberg, V.G. Zakrzewski, S. Dapprich, A.D. Daniels, M.C. Strain, O. Farkas, D.K. Malick, A.D. Rabuck, K. Raghavachari, J.B. Foresman, J.V. Ortiz, Q. Cui, A.G. Baboul, S. Clifford, J. Cioslowski, B.B. Stefanov, G. Liu, A. Liashenko, P. Piskorz, I. Komaromi, R.L. Martin, D.J. Fox, T. Keith, M.A. Al-Laham, C.Y. Peng, A. Nanayakkara, M. Challacombe, P.M.W. Gill, B. Johnson, W. Chen, M.W. Wong, C. Gonzalez, J.A. Pople, *Gaussian 03*, Revision D.01, Gaussian, Inc., Wallingford, CT, 2005.